DeepArc: Modularizing Neural Networks for the Model Maintenance

Xiaoning Ren[1], Yun Lin[2*], Yinxing Xue[1*], Ruofan Liu[3], Jun Sun[4], Zhiyong Feng[5], Jin Song Dong[3]
[1] University of Science and Technology of China, China, hnurxn@mail.ustc.edu.cn, yxxue@ustc.edu.cn
[2] Shanghai Jiao Tong University, China, lin_yun@sjtu.edu.cn
[3] National University of Singapore, Singapore, e0134091@u.nus.edu, dcsdjs@nus.edu.sg
[4] Singapore Management University, Singapore, junsun@smu.edu.sg
[5] Tianjin University, China, zyfeng@tju.edu.cn

***Abstract*—Neural networks are an emerging data-driven programming paradigm widely used in many areas. Unlike traditional software systems consisting of decomposable modules, a neural network is usually delivered as a monolithic package, raising challenges for some maintenance tasks such as model restructure and re-adaption. In this work, we propose DeepArc, a novel modularization method for neural networks, to reduce the cost of model maintenance tasks. Specifically, DeepArc decomposes a neural network into several consecutive modules, each of which encapsulates consecutive layers with similar semantics. The network modularization facilitates practical tasks such as refactoring the model to preserve existing features (e.g., model compression) and enhancing the model with new features (e.g., fitting new samples). The modularization and encapsulation allow us to restructure or retrain the model by only pruning and tuning a few *localized* neurons and layers. Our experiments show that (1) DeepArc can boost the runtime efficiency of the state-of-the-art model compression techniques by 14.8%; (2) compared to the traditional model retraining, DeepArc only needs to train less than 20% of the neurons on average to fit adversarial samples and repair under-performing models, leading to 32.85% faster training performance while achieving similar model prediction performance.**

***Index Terms*—architecture, modularization, neural networks**

I. Introduction

Deep neural network (DNN) models have attracted increasing attention in both industry and academia, widely incorporated in many modern software systems [1]–[6]. As a new programming paradigm, neural network models are programmed with predefined structures of mathematical functions [7], [8], whose parameters are learned automatically to fit a given training dataset. While a network model can be learned to function well, its hundreds of thousands of stacked "tiny functions" make it hard to interpret how the decisions are made, which in turn makes model maintenance challenging.

In practice, a trained DNN model needs to evolve with new requirements. Analogous to code logic modification and redundant code refactoring in traditional software, programmers and data scientists need to adapt the model regarding the new samples, or prune the model while preserving its behaviors (e.g., adapting a functional model into mobiles or IoT devices). However, existing practice usually requires retraining the model with the new and existing training dataset [9], which induces large maintenance costs. Note that classical neural networks usually consist of millions of weights (Resnet-50 [10] has about 25.6 million weights, VGGNet19 [11] has 143 million weights, and the emerging GPT-3 [12] even has 175 billion weights), which makes the current practice to maintain the models computationally expensive.

For the maintenance of DNN models, there are emerging works in SE community to decompose a model for improving its *reusability*. Pan et al. proposed to decompose a multi-classification model into a set of binary classification models for fully connected networks [13] and convolutional networks [14]. Technically, given a network model G and predication class set C, their solution extracts a subgraph $G' \in G$ as a binary classifier to preserve the behavior of G on C' ($C' \subset C$). However, this technique can provide limited support if we need to restructure the model G while preserving its behaviors or improve G's performance with minimum modifications.

In this work, we aim for a model modularization solution focusing on the *encapsulation* nature. Specifically, we investigate whether we can change only a few modularized neurons and layers in the model maintenance tasks. We propose to extract the *semantic architecture* of a neural network by encapsulating consecutive model layers as a *semantic module*. In a semantic module, (1) all layers extract features with similar expressiveness/separability for training/testing samples, and (2) some layers can be removed and duplicated without changing much model behavior (e.g., model prediction and robustness).

Those properties can facilitate applications such as model compression and model enhancement. The network modularization provides the following maintenance benefits:

- **Decomposition Overview**: By encapsulating similar layers, we can have an abstract view on how many *actual* transformation functions a network model can be decomposed. Each actual transformation (i.e., semantic module) is essentially a modularized feature-extraction subfunction.
- **Modularized Restructure**: Similar layers indicate potential redundant layers, which provides us the flexibility to remove and add some layers in a module without changing much model behavior.
- **Modularized Re-adaption**: Each semantic module can represent a unique feature-extraction function, which allows us to localize and retrain a certain critical module (instead of

* Yun Lin and Yinxing Xue are the corresponding authors.

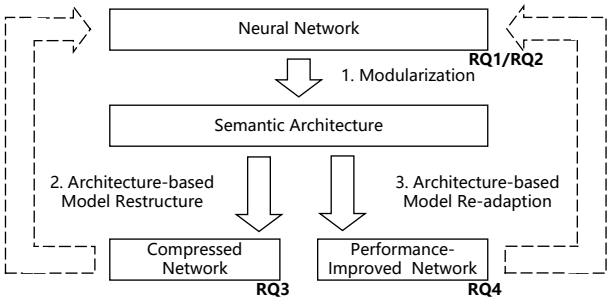

Fig. 1: Overview of DeepArc Framework

(a) Embedding Landscape 1 (b) Embedding Landscape 2 (c) Embedding Landscape 3

Fig. 2: Example of Embedding Landscape: For the sake of illustration, we use two-dimensional space in the examples.

the whole model) to either adapt to new samples or improve the performance on some mispredicted samples.

In this light, we propose, DeepArc, a modularization technique to extract the semantic architecture of a neural network, by encapsulating layers with similar *semantics*. Based on the modularized results, DeepArc can facilitate pruning model layers for model compression and localizing critical modules for model repair. Our extensive experiments show that DeepArc can boost the runtime efficiency of the state-of-the-art model compression techniques by 14.8%. Moreover, compared to the traditional model retraining, DeepArc only needs to fine-tune less than 20% of the neurons in the model to fit adversarial samples and repair under-performing models, leading to 32.85% faster training performance while achieving similar model prediction performance.

To summarize, we make the following contributions:

- We propose to extract semantic architecture to facilitate model maintenance tasks:
  - **Model restructuring task**: We improve the model compression efficiency by pruning the localized intra-module layers.
  - **Model re-adaption task**: We improve the model training efficiency by retraining the localized modules instead of the whole neural network.
- We publish our DeepArc framework, implemented for supporting the state-of-the-art deep models including both fully connected and convolutional layers.
- Our extensive experiments confirm the usefulness of semantic architecture on various model restructuring and re-adaption tasks.

II. DeepArc Framework

Figure 1 shows an overview of our DeepArc framework. Given a DNN model, DeepArc first extracts several modules to form a semantic architecture, each of which includes semantically similar model layers. Based on the semantic architecture, we can support (1) model restructure to modify the network while preserving its behaviors, and (2) model re-adaption to fix mis-prediction or fit a model on new samples. Moreover, the restructured or improved DNN can be further modularized to support new model restructuring or re-adaption tasks.

A. Semantic Architecture

Typically, a neural network can be decomposed into a sequence of network layers, i.e., $f_n(\cdot) = l_n(l_{n-1}(...l_1(\cdot)))(n > 1)$, where each subfunction $f_i(\cdot)(i > 1)$ takes the output of its former subfunction $f_{i-1}(\cdot)$ as input. We denote each layer as $l_i(\cdot) : \mathbb{R}^{n_{i-1}} \rightarrow \mathbb{R}^{n_i}$ where n_i and n_{i-1} are the number of neurons in l_i and l_{i-1} respectively. Given an input $x \in \mathbb{R}^{in}$ and a network $f_n(\cdot)$ with n layers, $f_n(\cdot)$ can generate $n-1$ representations each of which is the output of $f_i(\cdot) = l_i(l_{i-1}(\cdots l_1(\cdot)))(2 \leq i \leq n)$.

a) Layer Similarity: Given a dataset $D = \{x_1, \cdots x_m\}$, we denote $x_j \in D$ as an input and $f_i(x_j)$ as the output representation of x_j on layer l_i. With a similarity measurement on l_i, denoted as $sim_{l_i}(\cdot,\cdot)$, we call the matrix M_{l_i} as the *similarity matrix* of l_i where $M_{l_i}[p,q] = sim_{l_i}(x_p, x_q)$, p and q are the indexes of a pair of samples x_p and x_q. Therefore, the matrix at each layer has the same shape as $[m,m]$ and contains the similarity of all pairs of samples. Intuitively, M_{l_i} indicates the *embedding landscape* of dataset on the ith layer. Figure 2 demonstrates the embedding landscape of 16 data samples. Figure 2a and Figure 2b share similar landscape as the samples are in similar spatial distribution. Specifically, the data points share similar neighbours in the embedding space. In contrast, Figure 2a and Figure 2c share different landscape. A similar embedding landscape indicates that the model extracts similar semantics from the input samples. Typically, we implement $sim_{l_i}(\cdot,\cdot)$ as

$$sim_{l_i}(x_p, x_q) = f_i(x_p) \cdot f_i(x_q) \tag{1}$$

Further, given a dataset D and two layers l_i and l_j, we can define a *layer similarity measurement* $sim_{layer}(\cdot,\cdot) : (M_{l_i}, M_{l_j}) \rightarrow R^1$ with a range of $[0,1]$, to measure the similarity of the output representations of two layers. Following centered kernel alignment metrics [15], we implement $sim_{layer}(\cdot,\cdot)$ as:

$$sim_{layer}(M_{l_i}, M_{l_j}) = \frac{M_{l_i} \cdot M_{l_j}}{||M_{l_i}|| \cdot ||M_{l_j}||} \tag{2}$$

b) Module Similarity: Given a module p_k consisting of $m = |p_k|$ consecutive layers starting at l_{k_1}, i.e., $p = \{l_{k_1}, l_{k_2}, ..., l_{k_m}\}$ where $k_i(1 \leqslant i \leqslant m)$ denotes the index

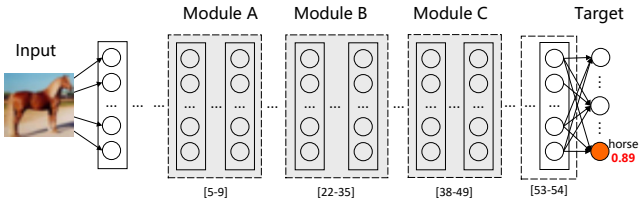

Fig. 3: An example of a modularized DNN for classification

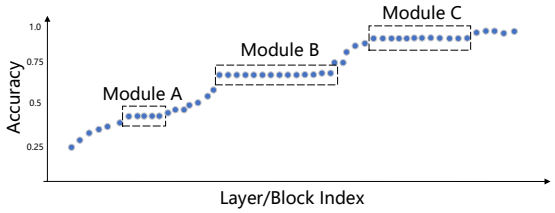

Fig. 4: Layers within the same modules share similar expressiveness: The x-axis represents layers, and y-axis represents the classification accuracy of a linear classifier trained on output representation of layers.

of the i-th layer in module p_k, we define the *intra-module similarity measurement* of p as:

$$sim_{module}(p_k) = \frac{\sum_{i=1}^{|p_k|-1} sim_{layer}(M_{l_{k_i}}, M_{l_{k_{i+1}}})}{|p_k| - 1} \quad (3)$$

If $|p_k| = 1$, we define $sim_{module}(p_k) = 0$. Intuitively, if the output representations of l_i and l_{i+1} are similar, the transformation of $f_{i+1}(\cdot)$ preserves the similar output (embedding) semantics as $f_i(\cdot)$. Moreover, we call a module p_k as *single-layer module* if $|p_k| = 1$; and call p_k as *multiple-layer module* if $|p_k| > 1$.

Given a network model $f_n(\cdot)$ and a similarity threshold th_s, the semantic architecture of $f_n(\cdot)$ is a partition $\mathcal{P}^*$ = {p_1, p_2, ..., p_M} (M is the number of modules) on a sequence of consecutive model layers so that

$$\max_{\mathcal{P}} \sum_{k=1}^{M} sim_{module}(p_k) - \sum_{\substack{l_i \in p_{k_1}, l_j \in p_{k_2}, \\ \forall p_{k_1} \in \mathcal{P}, p_{k_2} \in \mathcal{P}}} sim_{layer}(M_{l_i}, M_{l_j}) \quad (4)$$
$$\text{s.t.} \quad \forall p_k (|p_k| > 1), sim_{module}(p_k) > th_s$$

In Equation 4, the objective function requires that the overall layer similarity of each module in the partition is maximized while the layer similarity between different modules should be minimized. In addition, the condition requires that the overall layer similarity of each module in the partition should be larger than the predefined threshold th_s.

Example. Next, we use a RestNet-110 [10] model trained on CIFAR-10 [24] dataset to illustrate the modularization. The trained network has 54 blocks, which can be decomposed into 26 modules including multiple-layer and single-layer modules. Three largest multiple-layer modules are highlighted in Figure 3. Module A corresponds to 5-9th blocks, Module B corresponds to 22-35th blocks, Module C corresponds to 38-49nd blocks in ResNet-110. Specifically, Figure 3 shows an optimal partition $\mathcal{P}^* = \{\cdots, [5-9], \cdots, [22-35], \cdots, [38-49], \cdots, [53-54]\}$.

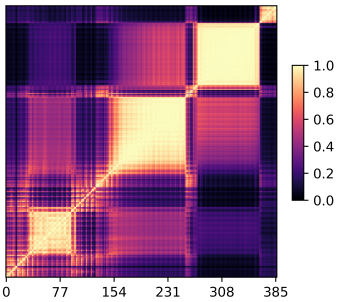

Fig. 5: Demonstration of the neighboring closeness of the layer similarity in neural network layers in ResNet-110.

Algorithm 1: Semantic Architecture Extraction

Input: sim, a layer-similarity matrix with shape (n, n) ($sim[i, j]$ indicates the similarity between two layers)
Input: th_s, a modular similarity threshold
Output: S_{layer}, a layer partition

```
module = ∅
for layer=1; layer≤n; layer++ do
    if module == ∅ then
        module = module ∪ {layer}
    else
        module' = module ∪ {layer}
        if sim(module') < th_s then
            S_layer = S_layer ∪ {module}
            module = {layer}
        else
            module = module ∪ {layer}
S_layer = S_layer ∪ {module}
return S_layer
```

Given a dataset D and a layer l_i, we say that D is $k\%$ linear separable on l_i if we can achieve a prediction accuracy of $k\%$ through training a logistic regression classifier to fit the output representation of D on l_i. The linear separability of layer l_i indicates how expressive the ith layer can be used to fit the dataset. Figure 4 demonstrates how the layers within a module are similar in expressing samples. Overall, the layers within a same module share similar expressiveness.

Layer Modularization. Equation 4 indicates the modularization (i.e., the search for an optimal partition) is an NP-complete problem, the global optimization is computationally expensive. We design our efficient modularization algorithm based on the observation of a phenomenon of *neighboring closeness* in neural network layers. Specifically, given layer i, $i + k_1$, and $i + k_2$ where $k_2 > k_1 > 0$, it is more likely that $sim_{layer}(l_i, l_{i+k_1}) > sim_{layer}(l_i, l_{i+k_2})$. Intuitively, closer layers go through less transformation, which are more likely to be similar. Figure 5 shows a visualized layer matrix where each row or column represents a layer and a matrix entry represents the similarity between two layers. The darker the

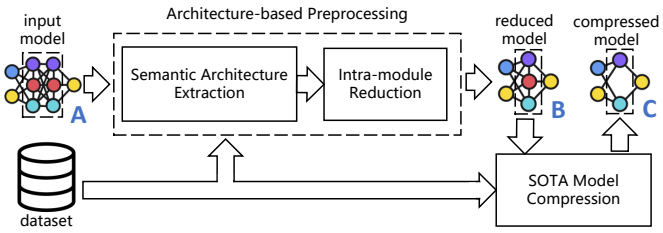

Fig. 6: An architecture-based acceleration for state-of-the-art model compression techniques.

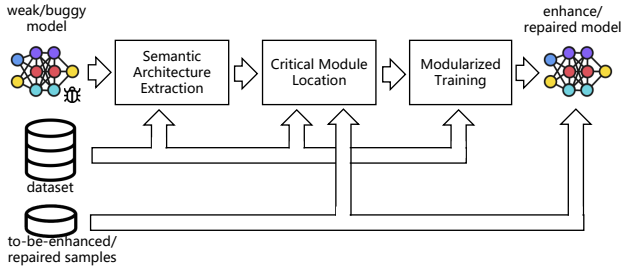

Fig. 7: An architecture-based model re-adaption approach

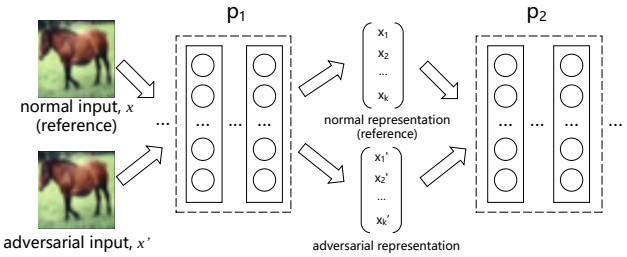

Fig. 8: Rationale of model re-adaption: (1) detecting a module where the representation of to-be-fixed samples deviates from that of normal samples (i.e., reference), and (2) training the localized module regarding the reference.

color, the smaller the similarity; the brighter the color, the larger the similarity.

Given that there is a high correlation between layer proximity and layer similarity, we design a progressive semantic architecture algorithm as a sub-optimal solution to Algorithm 1, which takes as input a layer-similarity matrix sim (as in Figure 5) and a modular similarity threshold (th_s), and generates a layer partition as the semantic architecture S_{layer}. We represent one network layer with its layer index, one network module as a set of layer indexes, and the semantic architecture as a set of modules. In Algorithm 1, we progressively merge the layers in sequential order (line 2). Specifically, we add a layer into a module if (1) the module is empty (line 3) or (2) the inner-module similarity of the to-be-merged module is above the threshold th_s. If a layer cannot be merged into the current module (line 7), we add the module into the semantic architecture, and create a new module for further analysis (lines 8-9). Overall, the complexity of Algorithm 1 is $O(n)$ where n is the model layer size.

B. Model Restructure

Given that the layers within a module share similar feature extraction, their "redundancy" can be used to reduce the model size. Some layers inside a module can be removed without modifying much of the model structure, while largely preserving the model behaviors such as prediction accuracy. Figure 6 shows our architecture-based model compression acceleration technique. Our architecture-based compression acceleration techique firstly obtains the reduced depth network B by removing the redundant network layers from network A, and then performs the standard compression technique to obtain network C. Larger granularity of pruning will lead to effective speedup. Overall, the extracted architecture serves as an informative guidance to prune redundant layers to have a pre-processed model. Then, the follow-up model compression techniques such as [16]–[20] can be applied to further fine-grained compression of the pre-processed model to drop the neurons/channels.

Layer Reduction. Given a module $p_k = \{l_{k_1}, l_{k_2}, ..., l_{k_n}\}$, for each layer l_{k_i}, we denote its input shape as $S_{in}(l_{k_i})$ and its output shape as $S_{out}(l_{k_i})$. Also, we denote the layer after the module is l_{next}. We reduce the module by keeping the first layer which acts as the interface layer, and removing the rest layers which represent redundant transformation information within the module. In the ideal case, $S_{out}(l_{k_i}) = S_{in}(l_{next})(1 \leq i \leq n)$, which means that we just need to "sew" the model by feeding l_{next} with the output of l_{k_i}. The smaller the value of i, the more model layers to remove. This lead to a static preprocessing way to prune the model, largely preserving the model behaviors. However, when $S_{out}(l_{k_i}) \neq S_{in}(l_{next})(1 \leq i \leq n)$, we need to introduce a "placeholder" layer to sew l_{k_i} and l_{next}, i.e., we have a sewing layer l_{sew} where $S_{in}(l_{sew}) = S_{output}(l_{k_i})$ and $S_{out}(l_{sew}) = S_{in}(l_{next})$. In this work, we locally train l_{sew} with the output representations of l_{k_i} and l_{k_n} as the input and output respectively. Specifically, we define loss function of l_{sew} by:

$$loss(p_k, l_{sew}) = ||l_{sew}(l_{k_i}(\cdot)), l_{k_n}(\cdots l_{k_i}(\cdot))||_2$$

From the perspective of software engineering, this sewing layer serves as a new interface between two modules.

C. Model Re-adaption

The model re-adaption includes enhancement and repair.

- **Model enhancement**: The model m is trained well on its original dataset D, while there is a requirement that m needs to perform well on new samples (e.g., adversarial samples).
- **Model repair**: The model m cannot perform well on a part of its original dataset. Thus, we need to retrain m on this part of dataset to achieve better performance.

Figure 7 shows an overview of our architecture-based model re-adaption technique, for both model enhancement and repair. The input of our technique is a model, the original training dataset, and a set of samples to be enhanced and repaired.

After achieving the semantic architecture, we apply a module-wise root-cause analysis technique to locate the most critical modules. Finally, we isolate the critical modules and apply traditional retraining process on them.

Rationale. The transformation between two module serves as the module interface. Suppose a module outputs a deviated representation from the "normal" representation, the deviation can cause all the follow-up modules to output unexpected representations, leading the model to make an unexpected prediction. Therefore, our approach aims to locate the most significant module where the representations of some samples are most deviated and fix it back to a normal representation.

Figure 8 shows an example where a normal input and its derived adversarial sample are fed into a modularized model. Taking the normal representation as a reference, we can retrain a single module (instead of the whole network) to correct the prediction. Therefore, the training can be applied in an *encapsulated* module instead of the whole network. Next, we introduce how to localize critical modules.

1) Critical Module Location: We locate the critical module by measuring the deviation of the new samples from the original dataset. Given a model m and its semantic architecture $\mathcal{P}^* = \{p_1, p_2, ..., p_n\}$, we know that m can be decomposed into n transformations. For each transformation (or module), we denote it as $\mathcal{M}_i : R^u \rightarrow R^v$, where R^u is the input space of the module and R^v is the output space. Given an input x, any module $\mathcal{M}_i$ can have its *input space representation*, denoted as $x_{\mathcal{M}_i^I}$ and *output space representation*, denoted as $x_{\mathcal{M}_i^O}$. In other words, $\mathcal{M}_i(x_{\mathcal{M}_i^I}) = x_{\mathcal{M}_i^O}$.

We assume that we have a dataset $\mathcal{D}$ where m can perform well and $\mathcal{D}'$ where m cannot perform well. For any module, taking its output space representation of $\mathcal{D}$ as a *reference*, we can evaluate the deviation of the representations of $\mathcal{D}'$ from that of $\mathcal{D}$. Our goal is to find a module where such deviation is significant, as the critical module for a re-adaption task. From the other perspective, we also identify the most non-robust features (or transformation) for its significant deviation.

Deviation Measurement. Let the dataset to be enhanced/repaired as $\mathcal{D}'$, We use $Dev(\mathcal{D}')$ as the deviation measurement for $\mathcal{D}'$. Given an input $\mathbf{x} \in D'$, we denote its deviation measurement as $Dev(\mathbf{x})$. We design different deviation measurements regarding explicit reference and implicit reference as follows.

- *Explicit Reference:* Given an dataset D', for each $\mathbf{x} \in D'$, if we can infer its *exact* ground truth output representation (denoted as $\mathbf{x}_{\mathcal{M}_i^O}$) in any modules, we call $D'_{\mathcal{M}_i^O}$ as the explicit reference of D'. For example, assuming that we know some adversarial inputs D' are derived from a normal dataset D, we can take the explicit reference $D_{\mathcal{M}_i^O}$ as $D'_{\mathcal{M}_i^O}$ (see Figure 8). Specifically, we use $sim_{layer}(\cdot, \cdot)$ distance between $D_{\mathcal{M}_i^O}$ and $D'_{\mathcal{M}_i^O}$ as $Dev(D')$.
- *Implicit Reference:* In contrast, if we need to *estimate* the ground truth output representation in any modules, we call the estimated ground truth as the explicit reference of $\mathbf{x}$. Intuitively, we estimate how likely $\mathbf{x}$ is to fall into the distribution of a subset of well-predicted dataset $\mathcal{D}_s \in \mathcal{D}$. For example, in a classification task, we estimate the probability that $\mathbf{x}$ can fall into the distribution of the sample set $\mathcal{D}_C \subset \mathcal{D}$ where (1) the label of each $\mathbf{s} \in \mathcal{D}_C$ is C, and (2) the model m can perform well on $\mathcal{D}_C$. Specifically, we estimate a multi-variable Gaussian probability distribution function $\mathcal{P}$ for $\mathcal{D}_C$, then calculate the probability of $\mathbf{x}$ being in the distribution of $\mathcal{D}_C$ by $\mathcal{P}(\mathbf{x})$. As a result, we use $\mathcal{P}(\mathbf{x})$ as $Dev(\mathbf{x})$ and $\frac{\sum_{\mathbf{x} \in \mathcal{D}'} Dev(\mathbf{x})}{|\mathcal{D}'|}$ as $Dev(\mathcal{D}')$.

2) Modularized Training: Given a critical module $\mathcal{M}$, we retrain the model by only fine-tuning the weights in $\mathcal{M}$. Given the original dataset $\mathcal{D}$, the to-be-adapted dataset $\mathcal{D}'$, and the to-be-adapted model m, we train m with the following loss function:

$$\mathcal{L}(\mathcal{D}, \mathcal{D}', model) = \alpha \cdot \mathcal{L}(\mathcal{D} \cup \mathcal{D}', model) + \beta \cdot Dev(\mathcal{D}') \quad (5)$$

In Equation 5, the first item $\mathcal{L}(\mathcal{D} \cup \mathcal{D}', model)$ is the original loss function to train a $model$. Note that the deviation measurements for explicit and implicit reference are differentiable. Intuitively, the deviation measurement can be regarded as an additional constraint (or soft invariant) forced by the "module interface". In addition, α and β are two user-defined hyperparameters.

III. Evaluation

We evaluate DeepArc with the following research questions:

- **RQ1 (Modularization Prevalence)**: To what extent can a neural network be modularized? Under what circumstances can and cannot the modularization disappear?
- **RQ2 (Modularization Semantics)**: What semantics can the layers in the same module share?
- **RQ3 (Model Restructure):** Can our architecture based model restructure technique effectively boost the state-of-the-art model compression tasks?
- **RQ4 (Model Re-adaption):** How effective is our architecture based model re-adaption technique that can improve the model retraining tasks?

RQ1 and RQ2 evaluate the effectiveness of our modularization method and the properties of the module itself. RQ3 and RQ4 evaluate the usefulness on two application tasks.

A. Dataset Setup

1) Model Architectures and Datasets: We choose the classical ResNet-110 [10], Wide-ResNet-38 [21], and VGGNet-19 [11] as the subject model architectures. In addition, we train the models on MNIST [22], FMNIST [23], and CIFAR-10 [24] datasets until the model performance converges. Moreover, we train each configuration (i.e., architecture-dataset combination) 10 times. We choose $th_s = 0.99$ (in Algorithm 1) to generate their semantic architectures. More detailed configurations (e.g., hyperparameters such as learning rate and decay ratio to train the models) can be referred to in [25].

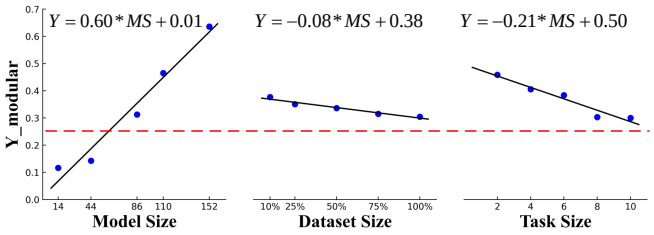

Fig. 9: Univariate linear regression analysis: The x-axis respectively represents the value of three variables and y-axis represents the modularity metric. For the five values of each univariate, there are 25 combinations of the other two variables and repeated 10 times, we can get 250 (5*5*10) values respectively, and then take the average. Horizontal red line reflect the high modularity threshold.

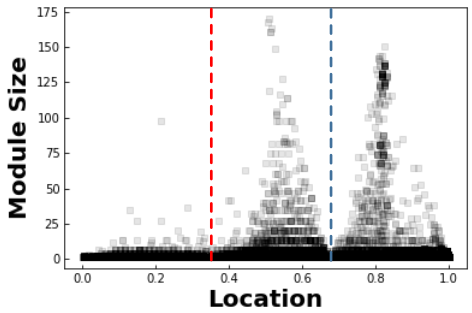

Fig. 10: Module distribution: The x-axis represents the location of modules in the models and the y-axis represents the module size (the number of layers in a module). Vertical red and blue lines reflect boundaries between ResNet stages, where the feature dimension changes.

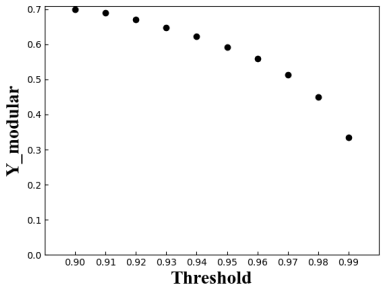

Fig. 11: The x-axis represents the threshold of modular algorithm and y-axis represents the degree of modularity.

B. Modularization Prevalence Experiment (RQ1)

1) Experiment Setup: To answer the RQ1, we design an experiment to observe the semantic architecture of a deep classifier by controlling three variables, i.e.,

- **Model Size (MS)**: The model architecture with different numbers of parameters. We take ResNet architecture [10] as the subject model because we can flexibly prune its size.
- **Dataset Size (DS)**: The datasets with different sizes. We take CIFAR-10 as the subject dataset and take 20%, 40%, 60%, 80%, 100% of the total samples in the experiment.
- **Task Scale (TS)**: Given an N-classification task, we choose five subsets of the task to control the classification task into $0.2N, 0.4N, 0.6N, 0.8N$ and N-classification.

The number of layers and parameters of the ResNet model includes five configurations of <14,0.176M>, <44,0.663M>, <86,1.34M>, <110,1.73M>, <152,2.42M>, each of which is trained 10 times on 5 dataset sizes and 5 task scales of CIFAR-10, with a total of 1250 (5*5*5*10) models.

Modularity Metrics. We define the *modularity metrics* $Y_{modular} = \frac{N^*_{layer}}{N_{layer}}$, indicating how modularized a model architecture is, and conduct a correlation analysis with $Y_{modular}$ as the dependent variable. In the metrics, N^*_{layer} is the number of layers in multi-layer modules and N_{layer} is the total number of layers. The fact that $Y_{modular} = 0$ means that the model has only *single-layer modules*, while the fact that $Y_{modular} = 1$ means all modules are *multiple-layer*. We define the high modularity threshold to be 1/4, which means that if over 1/4 of layers can be encapsulated, we think it can be effectively modularized. We further record the location of multi-modules to study the potential pattern of module distribution. Besides, to show the impact of the choice of threshold, we run our experiment with thresholds $th = 0.9, 0.91, 0.92, 0.93, 0.94, 0.95, 0.96, 0.97, 0.98, 0.99$ (see algorithm 1).

2) Results: Figure 9 shows the correlation analysis results of MS, DS, TS and $Y_{modular}$. The regression slope with the model size as the variable is positive and largest, while ones with the dataset and task are negative and relatively small. This shows that when the model size changes, it has the greatest impact on the modularity degree. Each independent variable has a certain correlation with the degree of modularity, in which DS and TS are negatively correlated with $Y_{modular}$, but MS positively. Considering all the variables together, a multivariate retrospective analysis yields a regression equation:

$$Y_{modular} = 0.78 * MS - 0.10 * DS - 0.16 * TS + 0.31 \quad (6)$$

This equation intuitively shows that $Y_{modular}$ has the highest sensitivity to model size, and relatively low sensitivity to dataset and task size, despite they all have a strong correlation. Besides, for popular configurations such as ResNet86 and ResNet110 on CIFAR-10, the high modularity threshold is exceeded, i.e. above the red line in the figure. In summary, the network modularity is usually present and particularly evident with a large model, simple task, and tiny data. In other words, the more redundant information the model has, the greater the degree of modularity. Typically, popular configurations can achieve effective modularity.

As shown in Figure 10, the *multiple-layer modules* are mainly found in the later layers of the model, because the features extracted later are more refined, and prone to redundant information due to slow feature transformation. Also, there are almost all *single-layer modules* on the boundary, where the feature dimension changes, usually acting as an interface

layer.

Besides, Figure 11 shows how the degree of modularity varies with the threshold th_s of algorithm 1. The threshold is a custom tradeoff, which needed to be set larger when we require a high level of information redundancy within the module, and vice versa. The threshold refers to the similarity of adjacent layers, and this similarity will become smaller as the layers are stacked. Therefore, we choose a threshold of 0.99 to guarantee a high degree of semantic similarity within modules.

Answer to RQ1: Usually, there is a modular phenomenon in the layers of the model. Model, dataset and task size will affect modularity and have a certain linear correlation. The modularization will almost disappear with a small model, complex task and huge dataset, that is, each layer is a module representing different semantics.

C. Modularization Semantics Experiment(RQ2)

To answer RQ2, we evaluate the semantic properties of the module in the following two parts:

- RQ2.1 (Dynamic Semantic): How much can the model behaviors change if we remove and replicate the layers in *multiple-layer modules*?
- RQ2.2 (Static Semantic): How much the prediction can vary if we use the intra/inter layers for the prediction?

1) Dynamic Semantics Design: We apply intra-module and inter-module changes on the models. We evaluate how the model prediction and robustness change when we remove and duplicate layers in intra-module and inter-module layers. Furthermore, in order to avoid introducing additional neurons when modifying the network model, we only add/remove the layers where the output dimension of their previous layer can match the input dimension of their following layer.

Intra-module Change. Given a trained model m and its derived semantic architecture $\mathcal{P}^* = \{p_1, \cdots, p_k\}$, where each p_i represents a module consisting of consecutive layers in m, we change m into its variant m' by removing or adding layers in multi-layer module p_i as follows.

We denote the original model as m_0, the model variant with k intra-module layers removed as m_{-k}, and that with k intra-module layers added as m_{+k}. Algorithm 2 shows the order we use to add and remove layers in the modules. Specifically, we sequentially parse the multi-layer modules in the semantic architecture (lines 2-3). For each module, we process its layer addition or removal from the last layer to its first layer (lines 4-7). Algorithm 2 provides a progressive way of adding and removing the layers.

Inter-module Change. Given a derived semantic architecture $\mathcal{P}^* = \{p_1, ..., p_k\}$, we can consider the layers in the single-layer modules as module interfaces. We remove them to have inter-model change. Their addition/removal order is the order they appear in the model.

Semantic Preserving Evaluation. Given the original model m_0 and its variant model $m_{+/-k}$, we evaluate how the semantics has been changed regarding the changed model prediction and robustness. We evaluate the model robustness change by how many adversarial samples for m_0 can be reused to compromise the model $m_{+/-k}$. Specifically, given an adversarial attack approach A, we generate N (N =1000 in the study) adversarial samples for m_0. If M out of N adversarial samples can still compromise $m_{+/-k}$, then we say that the model robustness change is $1 - \frac{M}{N}$. In this study, we use FGSM [26], DeepFool [27], C&W [28], and PGD [29] as adversarial attack approaches. Note that fine-tuning with few data is required for VGG19, while the ResNet family does not.

Algorithm 2: Layer Addition/Removal Order

Input: $\mathcal{P}*$, a semantic architecture $\mathcal{P}* = \{p_1, p_2, ..., p_k\}$
Output: $order(\cdot) : index \rightarrow order$, mapping each layer index to its order to be removed or added

```
1 o = 1
2 for i = 1; i <= k; i++ do
3     if p_i is multi-layer module then
4         for j = 1; j < |p_i|; j++ do
5             layer = last j layer in p_i
6             order(layer) → o
7             o = o + 1
8 return order(·)
```

2) Results of Dynamic Semantics: Figure 12 and Figure 13 show how the semantics are preserved for the model variants under different model architectures (i.e., ResNet-38, ResNet-110, and VGGNet-19). Given the space limit, we only show diversified model architectures on the CIFAR-10 dataset. More details and figures are available at [25]. Overall, the other two datasets (and with more training trials) share similar effects.

Preserving Model Prediction. In Figure 12, the x-axis shows the model variants caused by adding or removing k intra-module layers according to Algorithm 2. For example, "0" represents the original model, "-3" represents the model variant by removing 3 layers, and "8" represents the model variant by adding 8 layers. In the following, we denote a model by adding k layers as $k-$model. We can see that, the model prediction performance on both the training and testing dataset is largely preserved even if a large number of intra-module layers are removed. Besides, the same magnitude of variation indicates that changes within the module will preserve the model prediction ability, not causing overfitting or underfitting.

Preserving Robustness. Figure 13 shows the performance of model variants on the adversarial samples compromising the original model. Note that, the accuracy of 0-model is the performance of the original model on those adversarial samples. Except for FGSM, almost all the attacks make the accuracy of the original model drop to almost 0. We can see that the adversarial samples of different attack methods have different semantic preserving effects. Overall, the adversarial samples from PDG and FGSM can still compromise the model variants regardless of the number of added/removed layers. In contrast, there is a "jump" of prediction accuracy from 0-model to 1-model and -1-model for the adversarial samples from DeepFool and C&W (see the red and purple lines). Our

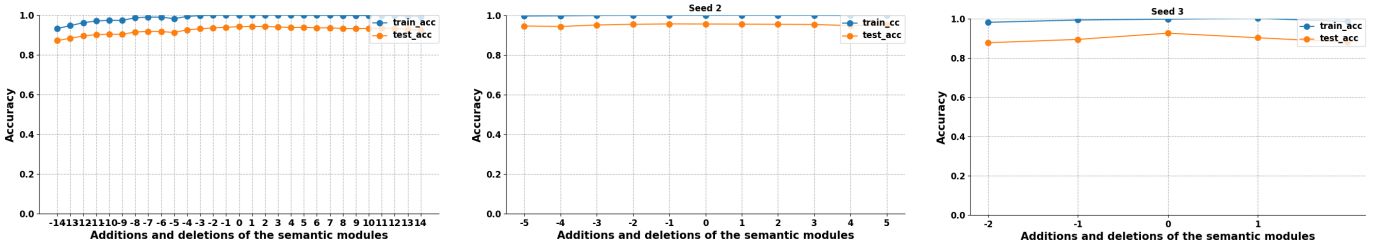

(a) ResNet110 (b) Wide-ResNet38 (c) VGGNet19

Fig. 12: Training and testing accuracy by removing and adding intra-module layers.

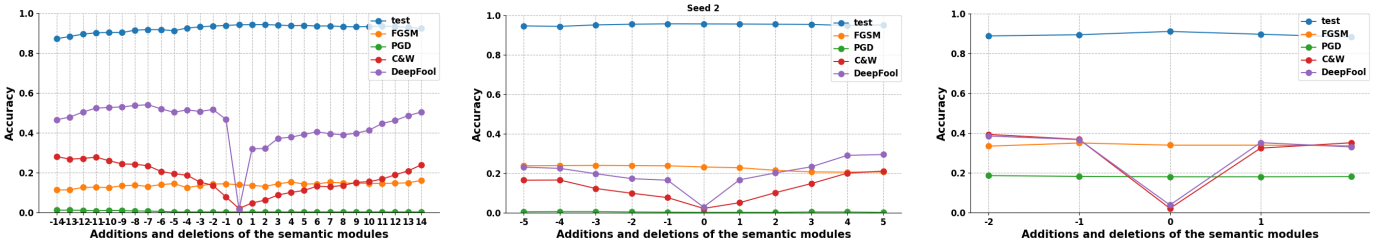

(a) ResNet110 (b) Wide-ResNet38 (c) VGGNet19

Fig. 13: The demonstration of how the adversarial samples for the original model can further compromise its model variants by removing/adding intra-module layers.

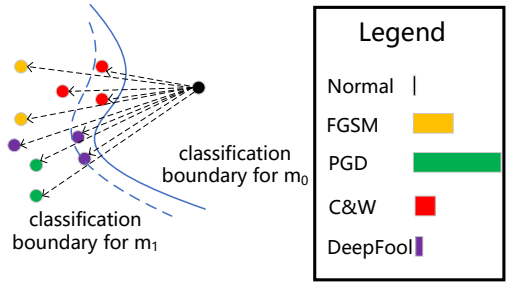

Fig. 14: Different adversarial samples, the distribution of different adversarial samples is different, which makes some samples fail to compromise the model variants.

investigation shows that, compared to the samples from PDG and FGSM, that from DeepFool and C&W are more likely to lie closer to the classification decision boundaries. The average model confidence score (the difference between the top-2 prediction before the softmax layer) on the adversarial samples of DeepFool is 2.38; in contrast, FGSM is 9.4 and PGD is 25, far larger than that of DeepFool. Figure 14 shows an illustration. Each deep classifier has its high-dimensional classification boundary (the solid curve in Figure 14), and its mutant can be considered as a perturbation of the boundary (the dashed curve in Figure 14). If some adversarial samples lie close to the boundary, the boundary perturbation can lead to the prediction change. Although the impact of deleting/adding one layer is very small, the boundary samples are sensitive to the layer change. Hence, DeepFool and C&W (with adversarial samples generated on the boundary) have larger performance changes while others have not.

Interface Importance. Figure 15 shows the change of testing accuracy if we gradually remove inter-module layers, compared to the removal of intra-module layers. For example, for the ResNet-110 architecture (Figure 15a), the model accuracy drops from 0.96 to 0.1, with the inter-module layer removal. In contrast, the model accuracy is still preserved around 0.9. This shows that the interface is responsible for transforming useful information. If the interface is broken, the overall information will be greatly affected.

Finding 1: The intra-module change can essentially preserve the semantics, regarding both model prediction and model robustness. However, the inter-module change can cause the model semantics to change radically.

3) Static Semantics Design: We quantify the static semantics of a layer l by how sufficient the output representation of l can be used to classify a training dataset *linearly*. Given a layer $\mathcal{L}$, and a dataset $\mathcal{D}$, we use $\mathcal{D}_{\mathcal{L}}$ to represent the set of output representation of $\mathcal{D}$ on $\mathcal{L}$. Specifically, we use a linear classifier (i.e., we use one linear-layer neural network in this work) to classify $\mathcal{D}_{\mathcal{L}}$ and achieve its classification accuracy, denoted as $Acc_{linear}(\mathcal{L})$. Intuitively, we measure the *linear expressiveness* of each layer to distinguish $\mathcal{D}$.

Linear Expressiveness Evaluation. Given an architecture as $\mathcal{P}^* = \{p_1, p_2, ..., p_n\}$, we sample N intra-module layer pair set $\mathcal{P}_{intra} = \{(\mathcal{L}_i, \mathcal{L}_j) | \ \mathcal{L}_i \in p_k, \ \mathcal{L}_j \in p_k, \ p_k \in \mathcal{P}^*$, and $i \neq j\}$; and N inter-module layer pair set $\mathcal{P}_{inter} = \{(\mathcal{L}_i, \mathcal{L}_j) | \ \mathcal{L}_i \in p_{k_1}, \ \mathcal{L}_j \in p_{k_2}, \ p_{k_1}, p_{k_2} \in \mathcal{P}^*, \ k_1 \neq k_2$, and $i \neq j\}$. For each $p = (\mathcal{L}_i, \mathcal{L}_j)$, we calculate the distance of linear expressiveness by $dis_{exp}(p) = |Acc_{linear}(\mathcal{L}_i) - Acc_{linear}(\mathcal{L}_j)|$. Then, given a model and its semantic architecture, we compare

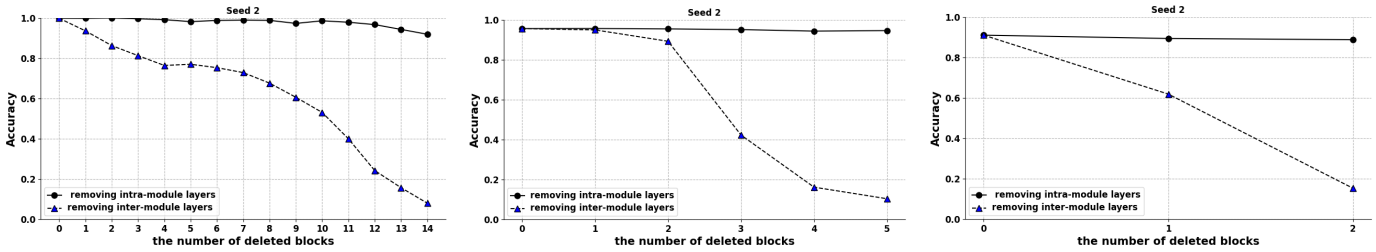

(a) ResNet110 (b) Wide-ResNet38 (c) VGGNet19

Fig. 15: Testing accuracy by removing intra-module layers, compared to the testing accuracy by removing inter-module layers

TABLE I: The difference of linear expressiveness of inter-module layers and intra-module layers

Dataset	Wide-ResNet38		ResNet110		VGGNet19	
	P_Intra	P_Inter	P_Intra	P_Inter	P_Intra	P_Inter
MNIST	0.044±0.001	0.217±0.006	0.026±0.001	0.161±0.003	0.063±0.001	0.252±0.008
FMNIST	0.017±0.002	0.123±0.008	0.015±0.000	0.104±0.002	0.056±0.002	0.130±0.009
CIFAR-10	0.077±0.001	0.246±0.002	0.012±0.001	0.220±0.000	0.002±0.000	0.201±0.009

the average and standard deviation of the difference in linear expressiveness of $\mathcal{P}_{intra}$ and $\mathcal{P}_{inter}$.

4) Results of Static Semantics: Table I shows that the linear expressiveness of intra-module layers is much more similar than that of inter-module layers. For the Wide-ResNet38 trained on MNIST, the average difference of the linear expressiveness of each intra-module layer is 0.044, while the average difference of each inter-module layer is 0.217. This shows that the difference score of inter-module linear expressiveness is nearly five times that of the difference score of intra-module linear expressiveness. On average, the difference score of intra-module linear expressiveness is 0.056, in contrast to that of inter-module linear expressiveness is 0.18. For the layers within the modules, the semantic transformations between them are more redundant and bring little help to the classification task.

Finding 2: The intra-module representations of a semantic architecture have similar linear separability. In contrast, the inter-module representations have more obvious differences.

Answer to RQ2: We demonstrate the effectiveness of modularization from three properties, prediction, robustness, and linear expressiveness. These properties are largely preserved inside the multi-layer modules. However, interface changes bring completely different results, leading to a significant loss of semantics.

D. Compression Efficiency Experiment(RQ3)

1) Experiment Setup: To answer the RQ3, we select 4 state-of-the-art model compression techniques proposed in the last two years (i.e., LAMP [30], Global [31], Uniform+ [32] and ERK [33]) to see whether our DeepArc framework can speed up the model compression efficiency. Following the above four works, we use ResNet-101 trained on CIFAR-10 as the target model. We conduct controlled experiments according to whether our framework is used for pre-processing before compression. Specifically, we collect the compression rate, model accuracy and number of iterations under the premise of guaranteeing similar prediction accuracy. The three indicators are as follows, 1) compression rate: the proportion of compressed parameters 2) number of iterations: the number of iterations required to complete the compression 3) model accuracy: the accuracy of the model on testset.

TABLE II: The model compression performance with/without the acceleration of DeepArc

Compression Method	Compression Rate	Number of Iterations	Average Model Accuracy
Lamp	13.01%	8	93.24%
Lamp+DeepArc	13.90%(+0.89%)	7(-1)	92.99%(-0.25%)
Glob	13.43%	9	93.77%
Glob+DeepArc	14.53%(+1.10%)	7(-2)	92.65%(-1.12%)
Unif	26.23%	5	91.81%
Unif+DeepArc	27.14%(+1.11%)	5(-0)	92.36%(+0.55%)
Erk	26.23%	5	87.29%
Erk+DeepArc	29.79(+3.56%)	4(-1)	89.11%(+1.82%)

2) Results: Table II shows how DeepArc framework can help to accelerate model compression efficiency. Given 4 compression techniques, we take our DeepArc framework as pre-processing, and then give 8 compression results. As shown in the table, Lamp and Glob benefit from our framework by reducing the number of iterations required and increasing the compression ratio while maintaining a minimal loss of accuracy. The other two methods not only reduce the number of iterations but improve the accuracy. On average, our framework can reduce the number of iterations from 6.75 to 5.75 by 14.8%, while improving the accuracy and compression ratio a little, to 0.25% and 1.7%, respectively.

Overall pruning the model in such a statical way incurs little loss of accuracy, facilitating model compression.

Answer to RQ3: Based on the removal of redundant information in semantic modules, DeepArc accelerates model restructure efficiency significantly, while resulting in models with comparable compression ratios and model accuracy.

E. Model Re-adaption Experiment(RQ4)

1) Experiment Setup: To answer the RQ4, we design two tasks to see whether DeepArc can improve the re-training efficiency with little loss, compared to an entire training.

TABLE III: The model re-adaption performance with/without the acceleration of DeepArc

Re-adaption Type	Training Approach	Dropped Accuracy	WideResNet38				ResNet110				VGGNet19			
			Trained Model Size	Original Accuracy	Retraining Accuracy	Training Time (s)	Trained Model Size	Original Accuracy	Retraining Accuracy	Training Time (s)	Trained Model Size	Original Accuracy	Retraining Accuracy	Training Time (s)
Model Enhancement	Fully Training	/	56.07M	0.0751	0.9980	294.63	1.73M	0.924	0.9804	95.82	20.03M	0.1505	0.9992	24.17
	Modularized Training	/	7.38M		0.9974	158.21	0.13M		0.9595	64.75	9.44M		0.9986	18.29
Model Repair	Fully Training	10%	56.07M	0.8946	1.0000	762.01	1.73M	0.8992	1.0000	466.14	20.03M	0.8971	0.9805	139.50
		30%	56.07M	0.6870	0.9787	659.02	1.73M	0.7016	0.9693	464.43	20.03M	0.6687	0.9677	137.47
		50%	56.07M	0.4860	0.9999	710.53	1.73M	0.512	1.0000	471.12	20.03M	0.4850	0.9811	145.90
	Modularized Training	10%	7.82M	0.8940	0.9999	611.22	0.11M	0.8999	0.9999	312.07	1.77M	0.8974	0.9661	89.22
		30%	7.43M	0.6873	0.9998	602.27	0.13M	0.7011	0.9992	309.16	4.49M	0.6685	0.9281	91.43
		50%	5.54M	0.4864	0.9884	593.41	0.15M	0.5120	0.9764	305.55	4.72M	0.4850	0.9410	95.01

Model Enhancement Task. In this experiment, we use four adversarial attacks, i.e., DeepFool [27], C&W [28], FGSM [26], and PGD [29] to generate 1000 adversarial samples. We compare the retraining accuracy and efficiency between our modularized training approach and traditional approach. Both aim to force the original model to perform well on those adversarial samples.

Model Repair Task. In this experiment, given a trained model m, we mutate m by progressively replacing its model weights with random values until its training accuracy drops by about 10%, 30%, and 50%. For each mutation configuration (i.e., a model architecture, a dataset, and a dropping accuracy rate), we generate 3 model mutants. For each model mutant, we compare DeepArc with traditional model retraining regarding the retraining accuracy and efficiency.

2) Results: Table III shows how the modularized training technique in DeepArc framework helps to accomplish the model enhancement task (a.k.a., adversarial training task) and the model repair tasks. Note that the models are trained on CIFAR-10, more details are available at [25].

Model Enhancement Task. As shown in Table III, modularized training of ResNet110 reduces trained model size from 1.73M to 0.13M, and decreases training time by about 32.4% with 2.1% accuracy loss. Across all the models, modularized training can reduce training time by 41.8% on average with comparative accuracy. Overall, compared to fully training the whole model, DeepArc allows us to achieve comparable model enhancement performance by only training a small subset of neural layers.

Model Repair Task. In the model repair task, DeepArc achieves a similar performance boost as in model enhancement task. We can also see that, even trained with a localized modular, DeepArc allows us to successfully achieve on average 0.976 training accuracy and reduce training time by 23.9%.

Answer to RQ4: In summary, (1) model re-adaption tasks are not necessary to retrain the whole model, and (2) localized/modularized training can boost the training efficiency with little accuracy loss.

F. Threats to Validity

External Validity. Threats to external validity arise from that our experiments is conducted on three model architectures and three datasets. To mitigate the risk, we included three most popular model architectures in the computer vision domain. These models including fully connected layers, convolutional layers, residual blocks, etc., are therefore already widely representative for DNNs. In the future, we will conduct more thorough studies to evaluate whether the effectiveness of DeepArc can be generalized to more diversified model architecture such as Transformer and BERT in NLP domains.

Internal Validity. Threats to internal validity may arise from the randomness of model training. To mitigate this threat, we prepared 10 seeds to retrain the models for the experiment.

IV. Discussion

We have shown that the semantic architecture of DeepArc is designed to inform (1) the number of *actual* transformation operations in the network, (2) a hint to statically remove or add model layers without radically changing model semantics, and (3) modularized layers that can be *compressed* by model restructure and *attributed* by model re-adaption tasks, just like a function in the functional program that can be attributed by bug-fixing and feature-enhancement tasks.

Nevertheless, the modularization in this work is still in the grain of transformation operations. While it is useful for tasks like refactoring and performance enhancement, it is not sufficient for module reuse, in comparison with the software modules in the traditional system. In practice, there are still many problems to be solved in reuse tasks. For example, The existing methods for reuse [13], [14] aim to extract subnetworks, which change the model structure in a significant way. In this work, the module interfaces of the semantic architecture are mainly used for encapsulation and localized retraining. In future work, we will explore how to extract human-readable interfaces, so that we can facilitate module-level model reuse.

V. Related Work

A. Software Architecture Recovery

Researchers have investigated the software architecture recovery for decades. The solutions are generally based on clustering, where the similarity measurement is defined based on concerns, code hierarchy or information entropy, which include Comprehension-Driven Clustering (ACDC) [34], Architecture Recovery using Concerns (ARC) [35], Bunch [36], scaLable InforMation BOttleneck (LIMBO) [37], Weighted Combined Algorithm (WCA) [38], and Zone-Based Recovery (ZBR) [39]. Based on the recovered code architecture, programmers and architects can have a broader overview and

deeper insight into the software system. For example, Wong et al. use a design structure matrix (i.e., DSM) [40] to extract the architecture and suggest potential design violations.

Unlike traditional software systems, the deep learning network is simpler in architecture (i.e., a sequence of transformation operations) while much harder to interpret. Our DeepArc framework takes the first step towards the modularity of the network layers. Moreover, the usefulness of our recovered modularity is not limited to comprehension, it can also facilitate model restructuring and model re-adaption tasks.

B. Modularity of Neural Network

The research on the modularity of the neural network model remains relatively under-explored. Although there are many DNN-related works that introduces the concept of modules [41]–[46] in the AI community, these mainly focus on formulating some specific functional DNN components for better interpretability in some specific domains. There are emerging works in the SE community to decompose a neural network for improving the model reusability. Pan et al. propose to decompose a multi-classification model into a set of binary classification models for fully connected networks [13] and convolutional networks [14]. These works extract the same number of multiple sub-networks as categories, by removing and modifying nodes and edges in the neural network. However, these binary classifiers are not conducive to acceleration of training and inference due to the discrete nature of the sub-networks, which is especially costly for tasks with a particularly large number of categories. Besides, these techniques can provide limited support if we need to restructure the model while preserving its behaviors or improving performance with the minimum modifications. Our modular approach operates directly on model layers, scaling the depth of the network without affecting the acceleration. Yet, the approach is designed to tune the network itself rather than extract new networks, and hence it can help with the maintenance of the model itself.

VI. Conclusion and Future Work

In this work, we started a first attempt to encapsulate a monolithic DNN into several consecutive modules and investigate whether it can be beneficial. We propose the framework DeepArc which allows us to extract the semantic architecture of a DNN, facilitating applications such as model restructure and enhancement tasks. We show that the architecture has some properties, largely preserving the fitting, robustness and linear separability. Besides, the tasks like model compression, enhancement, and repair can largely benefit from the modularity of network layers. In the future, we will further explore whether DeepArc framework can help modular reuse.

Acknowledgment

This research is supported in part by the National Nature Science Foundation of China (grant No.61832014, No.61972373), the Basic Research Program of Jiangsu Province, China (BK20201192), the Minister of Education, Singapore (T1-251RES1901, T2EP20120-0019, MOET32020-0004), NUS-NCS Joint Laboratory for Cyber Security, Singapore, the National Research Foundation, Singapore, and Cyber Security Agency of Singapore under its National Cybersecurity Research and Development Programme (Award No. NRF-NCR_TAU_2021-0002) and A*STAR, CISCO Systems (USA) Pte. Ltd and National University of Singapore under its Cisco-NUS Accelerated Digital Economy Corporate Laboratory (Award I21001E0002). Dr. Xue's research is also supported by CAS Pioneer Hundred Talents Program.

References

[1] K. Madala, D. Gaither, R. Nielsen, and H. Do, "Automated identification of component state transition model elements from requirements," in 2017 IEEE 25th international requirements engineering conference workshops (REW). IEEE, 2017, pp. 386–392.

[2] A. Joulin and T. Mikolov, "Inferring algorithmic patterns with stack-augmented recurrent nets," Advances in neural information processing systems, vol. 28, 2015.

[3] H. Tong, B. Liu, and S. Wang, "Software defect prediction using stacked denoising autoencoders and two-stage ensemble learning," Information and Software Technology, vol. 96, pp. 94–111, 2018.

[4] Y. Pang, X. Xue, and H. Wang, "Predicting vulnerable software components through deep neural network," in Proceedings of the 2017 International Conference on Deep Learning Technologies, 2017, pp. 6–10.

[5] G. E. Dahl, J. W. Stokes, L. Deng, and D. Yu, "Large-scale malware classification using random projections and neural networks," in 2013 IEEE International Conference on Acoustics, Speech and Signal Processing. IEEE, 2013, pp. 3422–3426.

[6] X. Li, H. Jiang, Z. Ren, G. Li, and J. Zhang, "Deep learning in software engineering," arXiv preprint arXiv:1805.04825, 2018.

[7] K.-T. Yang, "Artificial neural networks (anns): a new paradigm for thermal science and engineering," Journal of heat transfer, vol. 130, no. 9, 2008.

[8] D. Fohr, O. Mella, and I. Illina, "New paradigm in speech recognition: deep neural networks," in IEEE international conference on information systems and economic intelligence, 2017.

[9] S. C. Hoi, D. Sahoo, J. Lu, and P. Zhao, "Online learning: A comprehensive survey," Neurocomputing, vol. 459, pp. 249–289, 2021.

[10] K. He, X. Zhang, S. Ren, and J. Sun, "Deep residual learning for image recognition," in Proceedings of the IEEE conference on computer vision and pattern recognition, 2016, pp. 770–778.

[11] K. Simonyan and A. Zisserman, "Very deep convolutional networks for large-scale image recognition," arXiv preprint arXiv:1409.1556, 2014.

[12] T. Brown, B. Mann, N. Ryder, M. Subbiah, J. D. Kaplan, P. Dhariwal, A. Neelakantan, P. Shyam, G. Sastry, A. Askell et al., "Language models are few-shot learners," Advances in neural information processing systems, vol. 33, pp. 1877–1901, 2020.

[13] R. Pan and H. Rajan, "On decomposing a deep neural network into modules," in Proceedings of the 28th ACM Joint Meeting on European Software Engineering Conference and Symposium on the Foundations of Software Engineering, 2020, pp. 889–900.

[14] ——, "Decomposing convolutional neural networks into reusable and replaceable modules," in Proceedings of the 44th International Conference on Software Engineering, 2022, pp. 524–535.

[15] S. Kornblith, M. Norouzi, H. Lee, and G. Hinton, "Similarity of neural network representations revisited," in International Conference on Machine Learning. PMLR, 2019, pp. 3519–3529.

[16] J. S. Rosenfeld, J. Frankle, M. Carbin, and N. Shavit, "On the predictability of pruning across scales," in International Conference on Machine Learning. PMLR, 2021, pp. 9075–9083.

[17] J. Diffenderfer and B. Kailkhura, "Multi-prize lottery ticket hypothesis: Finding accurate binary neural networks by pruning a randomly weighted network," arXiv preprint arXiv:2103.09377, 2021.

[18] J. Lee, S. Park, S. Mo, S. Ahn, and J. Shin, "Layer-adaptive sparsity for the magnitude-based pruning," arXiv preprint arXiv:2010.07611, 2020.

[19] J. Frankle, G. K. Dziugaite, D. M. Roy, and M. Carbin, "Pruning neural networks at initialization: Why are we missing the mark?" arXiv preprint arXiv:2009.08576, 2020.

[20] S. Hayou, J.-F. Ton, A. Doucet, and Y. W. Teh, "Robust pruning at initialization," arXiv preprint arXiv:2002.08797, 2020.

[21] S. Zagoruyko and N. Komodakis, "Wide residual networks," arXiv preprint arXiv:1605.07146, 2016.

[22] Y. LeCun, L. Bottou, Y. Bengio, and P. Haffner, "Gradient-based learning applied to document recognition," Proceedings of the IEEE, vol. 86, no. 11, pp. 2278–2324, 1998.

[23] H. Xiao, K. Rasul, and R. Vollgraf, "Fashion-mnist: a novel image dataset for benchmarking machine learning algorithms," arXiv preprint arXiv:1708.07747, 2017.

[24] A. Krizhevsky, G. Hinton et al., "Learning multiple layers of features from tiny images," 2009.

[25] N.A, "Deeparc," https://sites.google.com/view/deep-arc/, 2022, [Online; accessed 18-Mar-2022].

[26] I. J. Goodfellow, J. Shlens, and C. Szegedy, "Explaining and harnessing adversarial examples," arXiv preprint arXiv:1412.6572, 2014.

[27] S.-M. Moosavi-Dezfooli, A. Fawzi, and P. Frossard, "Deepfool: a simple and accurate method to fool deep neural networks," in Proceedings of the IEEE conference on computer vision and pattern recognition, 2016, pp. 2574–2582.

[28] N. Carlini and D. Wagner, "Towards evaluating the robustness of neural networks," in 2017 ieee symposium on security and privacy (sp). IEEE, 2017, pp. 39–57.

[29] A. Madry, A. Makelov, L. Schmidt, D. Tsipras, and A. Vladu, "Towards deep learning models resistant to adversarial attacks," arXiv preprint arXiv:1706.06083, 2017.

[30] J. Lee, S. Park, S. Mo, S. Ahn, and J. Shin, "Layer-adaptive sparsity for the magnitude-based pruning," arXiv preprint arXiv:2010.07611, 2020.

[31] A. Morcos, H. Yu, M. Paganini, and Y. Tian, "One ticket to win them all: generalizing lottery ticket initializations across datasets and optimizers," Advances in neural information processing systems, vol. 32, 2019.

[32] T. Gale, E. Elsen, and S. Hooker, "The state of sparsity in deep neural networks," arXiv preprint arXiv:1902.09574, 2019.

[33] U. Evci, T. Gale, J. Menick, P. S. Castro, and E. Elsen, "Rigging the lottery: Making all tickets winners," in International Conference on Machine Learning. PMLR, 2020, pp. 2943–2952.

[34] V. Tzerpos and R. C. Holt, "ACDC: an algorithm for comprehension-driven clustering," in Proceedings of the Seventh Working Conference on Reverse Engineering, WCRE'00, Brisbane, Australia, November 23-25, 2000. IEEE Computer Society, 2000, pp. 258–267. [Online]. Available: https://doi.org/10.1109/WCRE.2000.891477

[35] J. Garcia, D. Popescu, C. Mattmann, N. Medvidovic, and Y. Cai, "Enhancing architectural recovery using concerns," in 26th IEEE/ACM International Conference on Automated Software Engineering (ASE 2011), Lawrence, KS, USA, November 6-10, 2011, P. Alexander, C. S. Pasareanu, and J. G. Hosking, Eds. IEEE Computer Society, 2011, pp. 552–555. [Online]. Available: https://doi.org/10.1109/ASE.2011.6100123

[36] B. S. Mitchell and S. Mancoridis, "On the automatic modularization of software systems using the bunch tool," IEEE Trans. Software Eng., vol. 32, no. 3, pp. 193–208, 2006. [Online]. Available: https://doi.org/10.1109/TSE.2006.31

[37] P. Andritsos and V. Tzerpos, "Information-theoretic software clustering," IEEE Trans. Software Eng., vol. 31, no. 2, pp. 150–165, 2005. [Online]. Available: https://doi.org/10.1109/TSE.2005.25

[38] O. Maqbool and H. A. Babri, "Hierarchical clustering for software architecture recovery," IEEE Trans. Software Eng., vol. 33, no. 11, pp. 759–780, 2007. [Online]. Available: https://doi.org/10.1109/TSE.2007.70732

[39] A. Corazza, S. D. Martino, V. Maggio, and G. Scanniello, "Investigating the use of lexical information for software system clustering," in 15th European Conference on Software Maintenance and Reengineering, CSMR 2011, 1-4 March 2011, Oldenburg, Germany, T. Mens, Y. Kanellopoulos, and A. Winter, Eds. IEEE Computer Society, 2011, pp. 35–44. [Online]. Available: https://doi.org/10.1109/CSMR.2011.8

[40] S. Wong, Y. Cai, M. Kim, and M. Dalton, "Detecting software modularity violations," in Proceedings of the 33rd International Conference on Software Engineering, 2011, pp. 411–420.

[41] J. Andreas, M. Rohrbach, T. Darrell, and D. Klein, "Neural module networks," in Proceedings of the IEEE conference on computer vision and pattern recognition, 2016, pp. 39–48.

[42] S. Sabour, N. Frosst, and G. E. Hinton, "Dynamic routing between capsules," Advances in neural information processing systems, vol. 30, 2017.

[43] R. Hu, J. Andreas, M. Rohrbach, T. Darrell, and K. Saenko, "Learning to reason: End-to-end module networks for visual question answering," in Proceedings of the IEEE international conference on computer vision, 2017, pp. 804–813.

[44] B. Ghazi, R. Panigrahy, and J. Wang, "Recursive sketches for modular deep learning," in International Conference on Machine Learning. PMLR, 2019, pp. 2211–2220.

[45] G. E. Hinton, Z. Ghahramani, and Y. W. Teh, "Learning to parse images," Advances in neural information processing systems, vol. 12, 1999.

[46] R. Atefinia and M. Ahmadi, "Network intrusion detection using multi-architectural modular deep neural network," The Journal of Supercomputing, vol. 77, no. 4, pp. 3571–3593, 2021.